



**Al-Sibd Center**  
for Research and Scholarly Publishing

# Iraqi Journal of Nanotechnology

## synthesis and application

Journal Homepage : <https://publications.srp-center.iq/index.php/ijn>



## Synthesis and Characterization of Nickel Oxide Nanoparticles by Green as well as Chemical Routes and Comparisons their Properties

**Mostefe Khalid Mohammed, Abdulqadier Hussien Al khazraji**

Department of Chemistry, College of Education for Pure Science, University of Diyala , Diyala, Iraq

\*Corresponding author: Email address [abdulqadier.niama@uodiyala.edu.iq](mailto:abdulqadier.niama@uodiyala.edu.iq)

### Keywords:

NiO nanoparticles;  
Co-precipitation ;  
Capparis Spinosa extract ;  
BET ;  
and XRD .

### Abstract

Nickel Oxide (NiO) Nanoparticles (NPs) were obtained using chemical and Eco-Friendly methods, utilizing Caper leaves extract, NaOH, and nickel sulfate hexahydrate. First step Ni(OH)<sub>2</sub> NPs was obtained by adding NaOH solution dropwise to mixture the caper leaves extract and solution of Ni(SO<sub>4</sub>)<sub>2</sub>·6H<sub>2</sub>O. Then, calcination was done at 600 °C and 6 h for the Ni(OH)<sub>2</sub> NPs to produce NiO NPs. Different techniques such as X-Ray, FTIR, FE-SEM, EDX and BET have used to evaluate the physical features of grown samples. However, the XRD pattern confirmed that all the samples are contains only NiO phase with average crystallite sizes 46.62 nm and 19.12 nm for both eco-friendly and co-precipitation methods, respectively. FESEM image of the NiO NPs revealed to be spherical shape. The elements content by green synthesis was shown in the EDX results as (Ni = 64.3 Wt%, O= 24.6 Wt%) and by chemical method as (Ni = 66.3, O= 29.3). According to BET analysis, the specific surface area of prepared NiO NPs using chemical precipitation method was greater than that produced using an eco-friendly method.

### Introduction

The term "nanotechnology" describes the synthesis or use of particles with dimension(s) below the nanometer range, or one billionth of a meter [1]. Because of the distinct influences of tiny size effect, surface effect, and quantum size effect, NPs exhibit unique characteristics that greatly differ from those of the comparable bulk solid state [2]. Nickel (group II) and oxygen (group VI) from the periodic table of naturally occurring elements are combined to form an II-VI composite semiconductor known as nickel oxide nanoparticles. NiO is a P-type semiconductor transition metal oxide that is incredibly robust, has straight band gaps between 3.5–3.8 eV, and has the ability to display super-paramagnetic and super-antiferromagnetic features [3]. Due to their low cost, lack of toxicity, and environmental friendliness, Nickel oxide nanoparticles are of great interest. This

material is used in a wide range of applications, such as transparent conductive, chemical sensors, and resistive random access memory. Additionally, it is a well-researched material that can also be used as a positive electrode in batteries and as a hole transport layer in quantum dot light emitting devices [4]. The synthesis of the NiO NPs has been achieved using a variety of techniques, including co-precipitation, sol gel, and solvothermal procedures [5]. Green synthesis is one of the various chemical and physical techniques used to create nanomaterial, and it has caught the attention of many researchers. The reason is that this approach to green synthesis is straightforward, economical, necessitates less heat and energy, and is environmentally friendly. Caper plant leaf extract was utilized as a mediator to obtain NiO NPs. The purpose of this study is to synthesize NiO NPs using two different techniques: first, by chemical precipitation of cappariss spinosa plant leaf extract, and second, by using cappariss spinosa plant leaf extract [6]. Chemical precipitation is the process of turning a liquid into a solid by adding chemical agents, supersaturating the liquid, and then separating the precipitates from the liquid. It facilitates the mass production of pure nanoparticles because it only needs one step. It is a very helpful method that even helps purify water and provides a long-term solution or outcomes that produce long-lasting effects [7]. The present work reports the nickel oxide NPs synthesis by green route (Capparis Spinosa: chelating agent) and by chemical route (co-participation). The structural, surface area, morphological and the elemental composition properties were studied for comparisons.

## Materials and Methods

### Chemical and plant materials

Nickel (II) sulfate hexahydrate (99%), Sodium hydroxide (NaOH), (99%), ethanol (99%) and Distilled H<sub>2</sub>O were of analytical grade and were purchased from BDH Company, England. Capparis Spinosa plant was collected from the University of Diyala, Baquba.

### Preparation of Capparis Spinosa Plant extracts

(5.0 g) of fresh leaves from Capparis Spinosa have ground into a fine powder after being cleaned with tap water; then this was washed by deionized water. The fine powder of Capparis Spinosa is dissolved in 200 mL of deionized water and boiled for 30 minutes at 80 °C. The extract was then filtered using filter paper NO. 1 and stored in refrigerator at 4 °C for further studies [8].

### Preparation of Nickel Oxide Nanoparticles using Capparis Spinosa extract

Nickel salt NiSO<sub>4</sub>.6H<sub>2</sub>O (0.3g) was dissolved in 50 mL of deionized water. The solution of plant extract was added stepwise to the solution while stirring at (25 °C), the temperature of the solution was raised up to (80 °C), and the mixture of the salt solution and the leaf extract was then added dropwise to the NaOH (0.1M) solution to achieve an approximate pH of 14 while stirring continuously for an hour. Then the mixture was filtered, and the precipitate (Ni(OH)<sub>2</sub> NPs) was collected and dried in an oven at 80 °C for 4 hours. The product has calcined for six hours at 600 °C to produce nickel oxide nanoparticles (NiO) [8].

### Preparation of Nickel Oxide Nanoparticles using Co- participation

NiO NPs have synthesized using Nickel Sulfate Hexahydrate (NiSO<sub>4</sub>.6H<sub>2</sub>O). Nickel salt solution (0.3 g) dissolved in the deionized water (50 mL). Salt solution was stirred continuously while NaOH (0.1M) solution was added dropwise to achieve a pH of about 11. The nickel hydroxide nanoparticles (Ni(OH)<sub>2</sub>NPs) form a black precipitate was collected after a short period of time, and repeatedly washed with deionized H<sub>2</sub>O to obtain pH 7. Following that, black precipitate was dried at 80 °C for

16 hours. NiO nanoparticles were obtained after calcination of Ni(OH)<sub>2</sub> NPs at 600 ° C for 6 hours [9].

### Characterization

Structural studies of NiO nanoparticles prepared using Capparis Spinosa plant extract were recorded on a Siemens model D500, the XPERT-Pro diffractometer using Cu K $\alpha$  radiation source as X-ray ( $\lambda=1.5405$ ) at room temperature. ZEISS Sigma VP scanning electron microscopes are used For morphological analysis. FT-IR spectrum of NiO synthesized nanoparticles are gained at the University of Diyala /College of Education for Pure Science (Schimadzu Spectrophotometer/Japan). The elemental analysis of NiO NPs studies was performed by EDX, and TriStar 3000, Micromeritics Inc. measured the pore volume and specific surface area (SSABET).

### Results and discussion

#### FT-IR spectroscopy

Fig. 1, (a) and 1(b) shows the FT-IR spectra of (Ni(OH)<sub>2</sub> NPs using chemical and green routs. The FT-IR spectrum of Ni(OH)<sub>2</sub>-green nanoparticles (Fig. a) showed broad band at 3417 cm<sup>-1</sup> related to O–H stretching vibration, as well as the band at 1509 cm<sup>-1</sup> revealed the bending vibration for the OH of water molecules coordinate to nickel in the Ni(OH)<sub>2</sub>, weak band at 455 cm<sup>-1</sup> is related to Ni–O. Similarly, (Fig. c), shows the FTIR spectrum of the Ni(OH)<sub>2</sub>-chemical nanoparticles, the peaks at 3417 cm<sup>-1</sup>, 3641 cm<sup>-1</sup> and 1635 cm<sup>-1</sup> is for O–H stretching and bending vibrations, respectively, and a weak peak appeared at 516 cm<sup>-1</sup> for the Ni–O lattice vibration. Fig (1 b) showed band at 3240 cm<sup>-1</sup> assigned to the stretching of OH group and weak band at 1635 cm<sup>-1</sup> is due to the bending of OH, while peak at 2021 cm<sup>-1</sup> refers to SO<sub>4</sub> group [10],[11]. The FT-IR spectrum of NiO-green and NiO-chemical NPs is shown in Fig.2,(a) and (b). The absorption bands that showed at 3387 and 3417 cm<sup>-1</sup> corresponds to (O-H) stretching of water in the NiO-green and NiO-chemical NPs respectively, and the peak at 1627 cm<sup>-1</sup> is for (H<sub>2</sub>O) bending vibrations. The bands at 1211 and 1149 cm<sup>-1</sup> are related to (C=O) group of (CO<sub>2</sub>) that adsorbed on surface of NPs from plant extract for NiO-green and NiO-chemical NPs respectively. Furthermore, the significant absorption band at 450 cm<sup>-1</sup> is assigned to stretching vibrations of (Ni-O). The aforementioned results thus confirm the predicted structure and functional groups [12], [13],[14].

#### XRD Analysis

The structural and crystalline size of NiO-green NPs and NiO-chemical NPs were studied using XRD technique. Fig. 3,( a) and (b) shows the strong peak of NiO-green NPs and NiO-chemical NPs. XRD pattern shows many diffraction peaks at 2 $\theta$  of 37.46°, 43.49°, 44.68, 63.07°, 75.59°, 76.52°, and 79.57° related to Crystallography Open Database of NiO 96-101-0096 with cubic structural. [15], while XRD pattern of NiO-chemical NPs shown five diffraction peaks at 37.44°, 43.47°, 63.24°,75.61° and 79.62 , which also had a cubic structural association with the International center for diffraction data of NiO 98-009-0203[5]. The average of crystallite size for NiO-green NPs and NiO-chemical NPs were 46.62 nm and 19.12 nm respectively, which was calculated using Debye Scherrer equation

$$D = \frac{\kappa * \lambda}{\beta \cos\theta}$$

The crystalline domain size (D) to the peak's width at half its height ( $\beta$ ), quantitatively describes the broadening of a peak at a specific diffraction angle ( $\theta$ ). The Scherrer constant,  $\kappa$ , is typically considered to be 0.91 but can vary with the morphology of the crystalline domains. Depending on the kind of X-rays being used, the X-ray wavelength ( $\lambda$ ) is a constant and the dislocation parameter is then calculated;  $\delta = 1/D^2$  [16, 17].

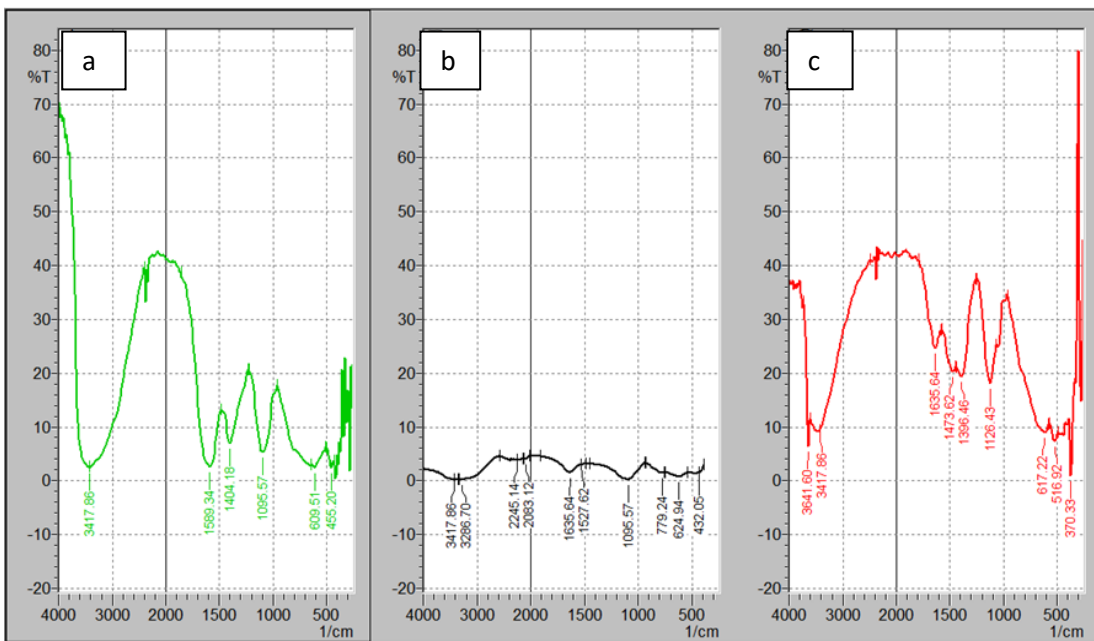


Fig .1, FTIR spectra of (a) Ni(OH)<sub>2</sub>-green nanoparticles, (b) NiSO<sub>4</sub>.6H<sub>2</sub>O and (c) Ni(OH)<sub>2</sub>-chemical nanoparticles.

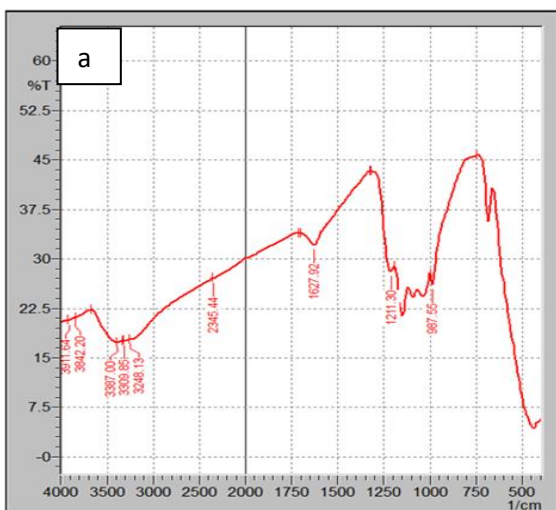


Fig 2. (a) FTIR spectra of NiO-green NPs.

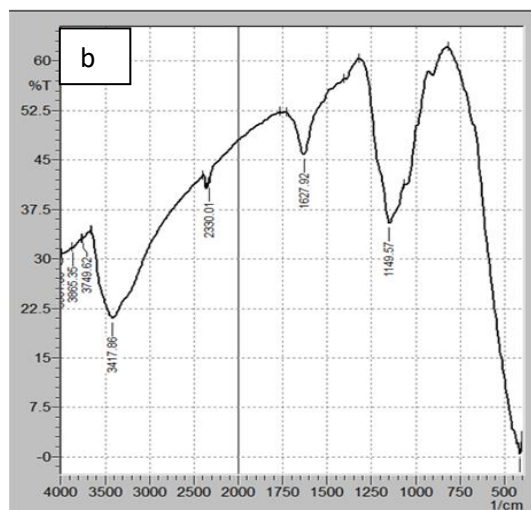


Fig 2. (b) FTIR spectra of NiO-chemical NPs.

Table 1. XRD data for NiO-Green NPs and NiO-Chemical.

Sample ID	2 $\theta$ ,Deg	FWHM ,nm	Dp, nm	dislocation parameter , $\delta$ ,1/d <sup>2</sup>	D Average ,nm	phase
a	20.8558	0.1968	42.90	0.00054361	46.62	NiO-green
	21.9521	0.1476	57.31	0.00030467		NiO-green
	22.9285	0.1968	43.05	0.00053982		NiO-green
	25.1847	0.1968	43.23	0.00053534		NiO-green
	26.9215	0.1968	43.39	0.00053164		NiO-green
	30.2458	0.2952	29.14	0.00117847		NiO-green
	31.3203	0.1968	43.82	0.00052125		NiO-green
	35.2854	0.1476	59.03	0.00028717		NiO-green
	37.4637	0.246	35.64	0.00078771		NiO-green
	38.8554	0.1968	44.74	0.00049980		NiO-green
	43.4956	0.246	36.34	0.00075765		NiO-green
	44.6849	0.1968	45.62	0.00048091		NiO-green
	45.6372	0.3936	22.89	0.00191024		NiO-green
	49.9245	0.1968	46.54	0.00046188		NiO-green
	50.3221	0.1968	46.62	0.00046049		NiO-green
	52.0377	0.246	37.56	0.00070921		NiO-green
	53.4456	0.3444	26.99	0.00137275		NiO-green
	55.3617	0.2952	31.76	0.00099137		NiO-green
	63.0752	0.3444	28.29	0.00125037		NiO-green
	66.9984	0.3936	25.30	0.0015635		NiO-green
72.9108	1.1808	8.74	0.013091	NiO-green		
75.5978	0.246	42.72	0.00054820	NiO-green		
76.5211	0.1476	71.65	0.00019484	NiO-green		
79.5778	0.1968	54.91	0.0003317	NiO-green		
b	35.1998	0.2952	29.51	0.0011490	19.12	NiO-chemical
	37.4444	0.5412	16.20	0.0038151		NiO-chemical
	43.4788	0.5904	15.14	0.0043626		NiO-chemical
	51.3982	0.5904	15.61	0.0041091		NiO-chemical
	62.9124	0.48	20.28	0.0024338		NiO-chemical
	63.2401	0.2952	33.03	0.0009171		NiO-chemical
	75.6134	0.6396	16.43	0.003704		NiO-chemical
	79.6248	0.492	21.97	0.0021061		NiO-chemical

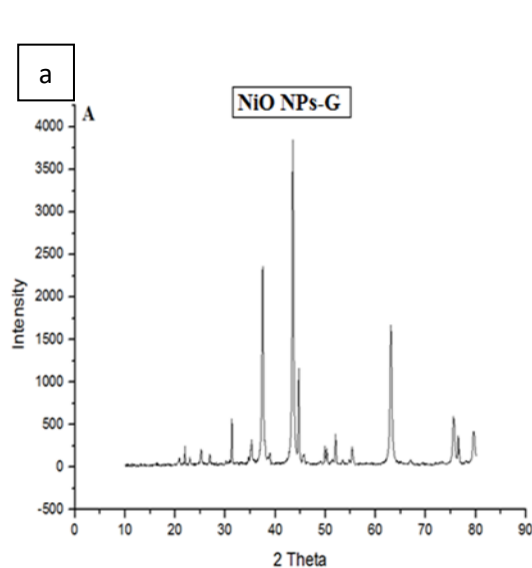


Fig 3. a XRD pattern of NiO-green NPs

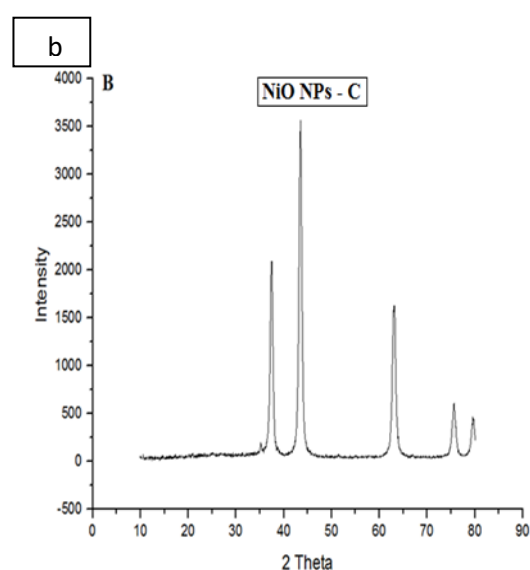


Fig 3.b XRD pattern of NiO-chemical NPs

## FESEM Results

FESEM is one of the well-recognized techniques to evaluate the morphology of nanomaterials. Fig (4a-b) show FESEM images of (a) Ni(OH)<sub>2</sub>-green NPs and (b) Ni(OH)<sub>2</sub>-chemical NPs. FESEM images of the Ni(OH)<sub>2</sub>-green NPs is shown in figure (4 a), which revealed irregular shape nanoparticles with agglomeration, average diameters 51.92 nm. However, when compared to the case of Ni(OH)<sub>2</sub>-green, the FESEM image of Ni(OH)<sub>2</sub>-chemical nanoparticles in figure (4 b) confirmed the presence of regular spherical shapes nanoparticles with average diameters of about 68.75nm [18]. The morphology of nickel oxide nanoparticles-green and chemical routes were examined using FESEM. The typical shapes of NiO- green NPs is shown in the Fig (4.c) and spheres, measuring approximately 58.47 nm, contain some tiny NiO nanoparticles. Fig. (4.d) provides the FESEM images of the NiO-chemical NPs product. They are almost spherical in shape. Thus, it is evident that the large spheres are made of various-sized small nanoparticles [19], [20].

## EDX Analysis

The results of the EDX analysis for the NiO NPs in Fig. 5a and b, shows that the obtained nanoparticles were composed from Ni and O elements. The element percentages that obtained from EDX were (66.8% and 68.5% of Ni, 16.3% and 19.2% of O) for NiO-green and NiO-chemical respectively. Peaks gold and molybdenum were derived from the initial stages of preparation for EDX observation [21]. The appearance of a peak at 0.2 due to the carbon atom produced by the filter paper residue, which showed the NiO formation with acceptable purity [22].

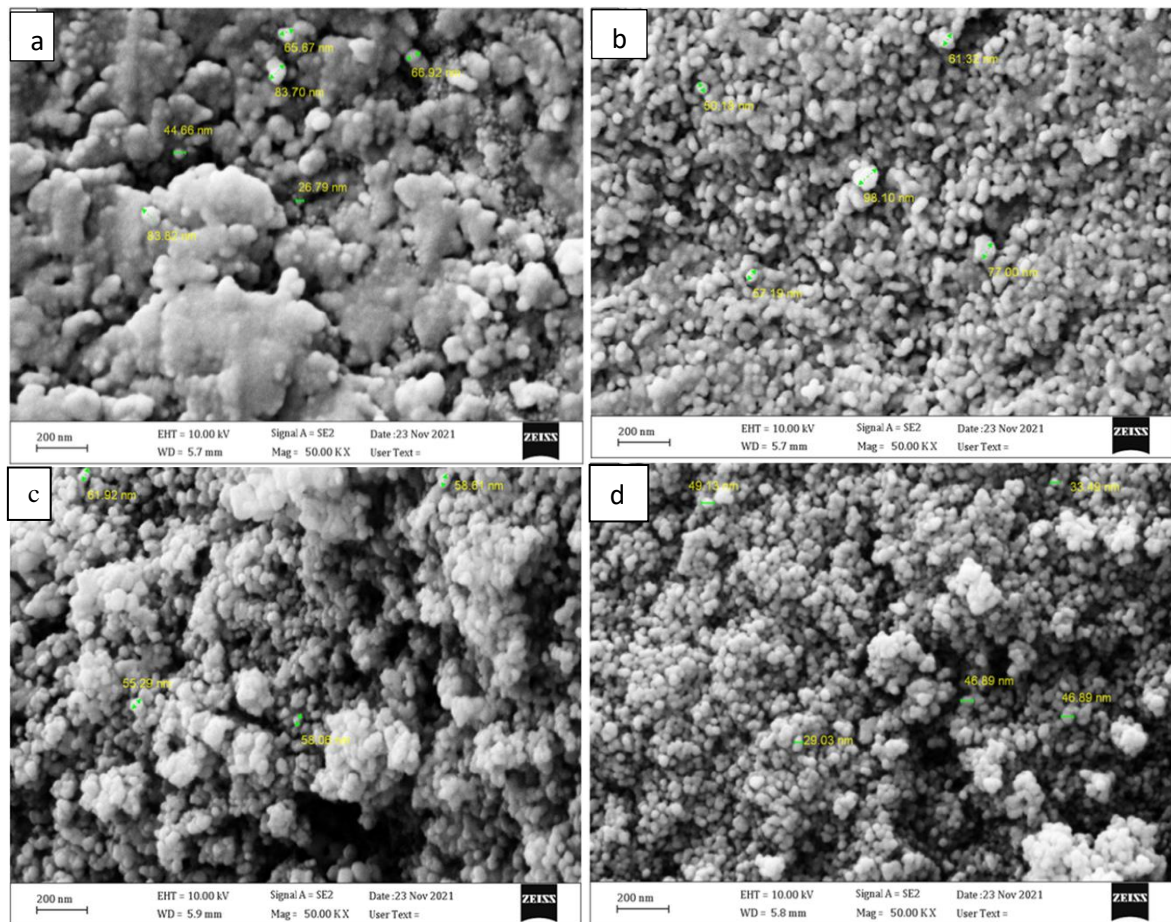


Fig 4. FESEM image of (a) Ni(OH)<sub>2</sub>-green, (b) Ni(OH)<sub>2</sub> chemical, (c) NiO-green, and (d) NiO-chemical route

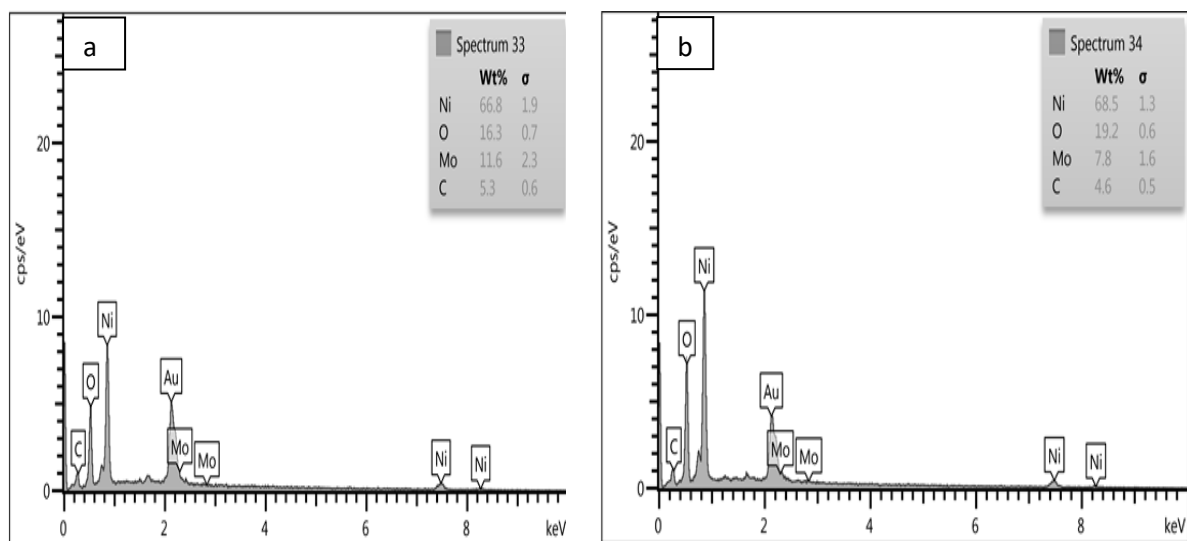


Fig 5. EDX Analysis of NiO NPs (a) green route and (b) chemical route .

### Brunauer–Emmett–Teller and Barrett, Joyner, and Halenda Analysis

The NiO NPs has analyzed via BET and BJH to absorb nitrogen gas at constant temperature of 77K. The specific surface area of the NiO-green NPs was obtained to be  $3.7671 \text{ m}^2/\text{g}$  with average pore diameter about  $26.881 \text{ nm}$  and total pore volume of  $0.025316 \text{ cm}^3/\text{g}$  (Fig.6 a). Mesopores (pores 5-55 nm in diameter) were detected in the NiO-green NPs according to a BJH diagram (Fig. 6 b), and it was also noticed that the pore size was irregular, with the majority of the nano pores falling within (5–20) nm range.

The NiO-chemical NPs' BET surface area, average pore diameter, and total pore volume, on the other hand, were calculated to be  $32.329 \text{ m}^2/\text{g}$ ,  $24.098 \text{ nm}$ , and  $0.1948 \text{ cm}^3/\text{g}$ , respectively (Fig. 6 c). NiO-chemical NPs were found to have mesopores, or pores that are between 2 and 55 nanometers in diameter, according to a BJH diagram (Fig. 6.d). It was also noted that the pore size was not uniform here, with the majority of the nano pores falling between 2 and 10 nanometers (Fig .6 d) [23].

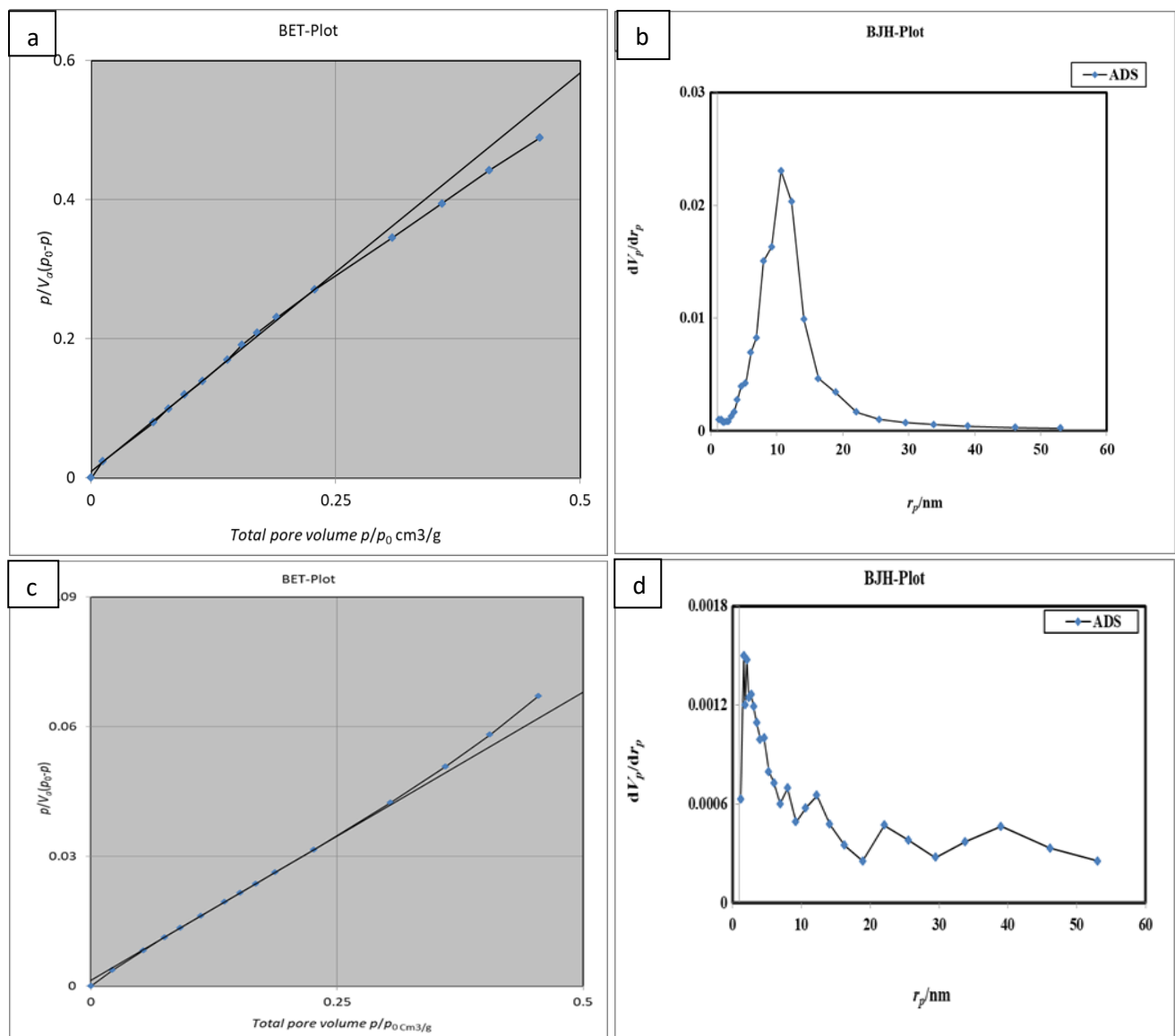


Fig 6. Surface area and distribution of pores of NiO- NPs, (a) BET curve of green route, (b) BJH plot of green route, (c) BET curve of chemical route and (d) BJH plot of chemical route



According to the study's findings, the mean size of NiO NPs were 46.62 and 19.12 nm for NiO-green NPs and NiO-chemical NPs respectively as determined by XRD technique. The BET technique of surface area for NiO nanoparticles is  $3.7671\text{m}^2/\text{g}$  and  $32.329\text{m}^2/\text{g}$  for NiO nanoparticles by green route and chemical route, respectively

### Conflicts of interest

The authors make it clear that they do not have any Conflicts of interest in this work.

### Formatting of funding sources

Funding sources are personal funds.

### Acknowledgment

The authors would like to thank the Faculty of Chemistry Science and University of Diyala for supporting this work.

### References

- [1] L. Singh, H. G. Kruger, G. E. M. Maguire, T. Govender, and R. Parboosing, "The role of nanotechnology in the treatment of viral infections," *Ther. Adv. Infect. Dis.*, vol. 4, no. 4, pp. 105–131, 2017.
- [2] H. Qiao, Z. Wei, H. Yang, L. Zhu, and X. Yan, "Preparation and characterization of NiO nanoparticles by anodic arc plasma method," *J. Nanomater.*, vol. 2009, 2009.
- [3] M. Hashem *et al.*, "Fabrication and characterization of semiconductor nickel oxide (NiO) nanoparticles manufactured using a facile thermal treatment," *Results Phys.*, vol. 6, pp. 1024–1030, 2016.
- [4] P. Dubey, N. Kaurav, R. S. Devan, G. S. Okram, and Y. K. Kuo, "The effect of stoichiometry on the structural, thermal and electronic properties of thermally decomposed nickel oxide," *RSC Adv.*, vol. 8, no. 11, pp. 5882–5890, 2018.
- [5] N. N. M. Zorkipli, N. H. M. Kaus, and A. A. Mohamad, "Synthesis of NiO nanoparticles through sol-gel method," *Procedia Chem.*, vol. 19, pp. 626–631, 2016.
- [6] G. T. Anand, R. Nithiyavathi, R. Ramesh, S. J. Sundaram, and K. Kaviyarasu, "Structural and optical properties of nickel oxide nanoparticles: Investigation of antimicrobial applications," *Surfaces and Interfaces*, vol. 18, p. 100460, 2020.
- [7] G. Sharma *et al.*, "J. King Saud Univ," *Sci*, vol. 31, pp. 257–269, 2019.
- [8] Thatoi, P., Kerry, R. G., Gouda, S., Das, G., Pramanik, K., Thatoi, H., & Patra, J. K. (2016). Photo-mediated green synthesis of silver and zinc oxide nanoparticles using aqueous extracts of two mangrove plant species, *Heritiera fomes* and *Sonneratia apetala* and investigation of their biomedical applications. *Journal of Photochemistry and Photobiology B: Biology*, 163, 311-318.
- [9] Hitkari, G., Sandhya, S., Gajanan, P., Shrivash, M. K., & Deepak, K. (2018). Synthesis of chromium doped cobalt oxide (Cr: Co<sub>3</sub>O<sub>4</sub>) nanoparticles by co-precipitation method and enhanced photocatalytic properties in the visible region. *J. Mater. Sci. Eng*, 7(419), 2169-2222.

- [10] J. Tientong, S. Garcia, C. R. Thurber, and T. D. Golden, "Synthesis of nickel and nickel hydroxide nanopowders by simplified chemical reduction," *J. Nanotechnol.*, vol. 2014, 2014.
- [11] P. E. Lokhande and H. S. Panda, "Synthesis and characterization of Ni. Co (OH) 2 material for supercapacitor application," *Synthesis (Stuttg.)*, vol. 2, no. 9, 2015.
- [12] Z. N. Kayani, M. Butt, Y. Ali, S. Riaz, and S. Naseem, "Structural and optical study of NiO nanoparticles," *Mater. Today Proc.*, vol. 2, no. 10, pp. 5804–5807, 2015.
- [13] P. Vijaya Kumar, A. Jafar Ahamed, and M. Karthikeyan, "Synthesis and characterization of NiO nanoparticles by chemical as well as green routes and their comparisons with respect to cytotoxic effect and toxicity studies in microbial and MCF-7 cancer cell models," *SN Appl. Sci.*, vol. 1, no. 9, pp. 1–15, 2019.
- [14] C. R. R. Kumar, V. S. Betageri, G. Nagaraju, G. H. Pujar, B. P. Suma, and M. S. Latha, "Photocatalytic, nitrite sensing and antibacterial studies of facile bio-synthesized nickel oxide nanoparticles," *J. Sci. Adv. Mater. Devices*, vol. 5, no. 1, pp. 48–55, 2020.
- [15] M. Wardani, Y. Yulizar, I. Abdullah, and D. O. B. Apriandanu, "Synthesis of NiO nanoparticles via green route using *Ageratum conyzoides* L. leaf extract and their catalytic activity," in *IOP Conference Series: Materials Science and Engineering*, 2019, vol. 509, no. 1, p. 12077.
- [16] Yousaf, S., Zulfikar, S., Shahi, M. N., Warsi, M. F., Al-Khalli, N. F., Aboud, M. F. A., & Shakir, I. (2020). Tuning the structural, optical and electrical properties of NiO nanoparticles prepared by wet chemical route. *Ceramics International*, 46(3), 3750-3758.
- [17] Ungar, T. J. S. M. (2004). Microstructural parameters from X-ray diffraction peak broadening. *Scripta Materialia*, 51(8), 777-781.
- [18] M. Halder, M. M. Islam, P. Singh, A. Singha Roy, S. M. Islam, and K. Sen, "Sustainable generation of Ni (OH) 2 nanoparticles for the green synthesis of 5-substituted 1 H-tetrazoles: a competent turn on fluorescence sensing of H<sub>2</sub>O<sub>2</sub>," *ACS omega*, vol. 3, no. 7, pp. 8169–8180, 2018.
- [19] G. Bharathy and P. Raji, "Room temperature ferromagnetic behavior of Mn doped NiO nanoparticles: a suitable electrode material for supercapacitors," *J. Mater. Sci. Mater. Electron.*, vol. 28, no. 23, pp. 17889–17895, 2017.
- [20] Z. Fereshteh, M. Salavati-Niasari, K. Saberyan, S. M. Hosseinpour-Mashkani, and F. Tavakoli, "Synthesis of nickel oxide nanoparticles from thermal decomposition of a new precursor," *J. Clust. Sci.*, vol. 23, no. 2, pp. 577–583, 2012.
- [21] Hashem, M., Saion, E., Al-Hada, N. M., Kamari, H. M., Shaari, A. H., Talib, Z. A., ... & Kamarudeen, M. A. (2016). Fabrication and characterization of semiconductor nickel oxide (NiO) nanoparticles manufactured using a facile thermal treatment. *Results in physics*, 6, 1024-1030.
- [22] Z. Sabouri, A. Akbari, H. A. Hosseini, M. Khatami, and M. Darroudi, "Egg white-mediated green synthesis of NiO nanoparticles and study of their cytotoxicity and photocatalytic activity," *Polyhedron*, vol. 178, p. 114351, 2020.
- [23] S. M. Roopan *et al.*, "Sunlight mediated photocatalytic degradation of organic pollutants by statistical optimization of green synthesized NiO NPs as catalyst," *J. Mol. Liq.*, vol. 293, p. 111509, 2019.